Possible manifestation of the $2p$ pionium in particle physics processes

Peter Lichard

Institute of Physics and Research Centre for Computational Physics and Data Processing, Silesian University in Opava, 746 01 Opava, Czech Republic and Institute of Experimental and Applied Physics, Czech Technical University in Prague, 128 00 Prague, Czech Republic

(Received 11 September 2020; accepted 29 September 2020; published 16 October 2020)

We suggest a few particle physics processes in which excited $2p$ pionium $A'_{2\pi}$ may be observed. They include the $e^+e^- \to \pi^+\pi^-$ annihilation, the $V^0 \to \pi^0\ell^+\ell^-$ and $K^\pm \to \pi^\pm\ell^+\ell^-$ ($\ell = e, \mu$) decays, and the photoproduction of two neutral pions from nucleons. We analyze available experimental data and find that they, in some cases, indicate the presence of $2p$ pionium, but do not provide definite proof.

DOI: 10.1103/PhysRevD.102.073004

I. INTRODUCTION

The first thoughts about an atom composed of a positive pion and a negative pion (pionium, or $A_{2\pi}$ in the present-day notation) appeared almost sixty years ago. Uretsky and Palfrey [1] assumed its existence and analyzed the possibilities of detecting it in the photoproduction off hydrogen target. Up to this time, such a process has not been observed. They also hypothesized about the possibility of decay $K^+ \to \pi^+ A_{2\pi}$, which has recently been observed in the experiment we mention below.

Pionium was discovered in 1993 at the 70 GeV proton synchrotron at Serpukhov, Russia [2]. The $A_{2\pi}$ atoms were produced in a Ta target and in the same target they broke-up into their constituents with approximately equal energies and small relative momenta, which distinguished them from the "free" $\pi^+\pi^-$ pairs.

Using a similar method, the properties of ground-state pionium were intensively studied in the Dimeson Relativistic Atomic Complex (DIRAC) experiment at the CERN Proton Synchrotron [3]. A careful analysis showed that the mean pionium lifetime is $\tau = 3.15^{+0.28}_{-0.26} \times 10^{-15}$ s. It decays into two neutral pions [1,4] and, to a much lesser extent, into two photons [5].

The NA48/2 [6] experiment at CERN Super Proton Synchrotron (SPS) observed a cusplike structure in the $\pi^0\pi^0$ invariant mass distribution from $K^\pm \to \pi^\pm\pi^0\pi^0$ decay. The enhancement can be interpreted as the contribution from the decays $K^\pm \to \pi^\pm A_{2\pi}$ (considered in [1]) followed by the decay $A_{2\pi} \to \pi^0\pi^0$ [7].

The DIRAC collaboration recently discovered [8] so-called long-lived $\pi^+\pi^-$ atoms. These objects are apparently excited $2p$ states of the ground-state pionium $A_{2\pi}$. The discovery was enabled by modifying the original DIRAC setup by adding a Pt foil downstream of the production Be target. The breakup of the long-lived states happened in that foil, placed at a distance of 96 mm behind the target. The magnetic field between the target and the foil does not influence the path of neutral atoms, but the $\pi^+\pi^-$ pairs coming from various sources are made more divergent.

The longevity of $2p$ pionium ($A'_{2\pi}$) is caused by the fact that its quantum numbers $J^{PC} = 1^{--}$ prevent it from decaying into the positive C-parity $\pi^0\pi^0$ and $\gamma\gamma$ states. It must first undergo the $2p \to 1s$ transition to the ground state. The mean lifetime of $2p$ pionium

$$\tau_{2p} = 0.45^{+1.08}_{-0.30} \times 10^{-11} \text{ s}. \tag{1}$$

is close to the value which comes for the $\pi^+\pi^-$ atom assuming a pure Coulomb interaction [8]. After reaching the 1s state, a decay to two π^0s quickly follows: $A'_{2\pi} \to A_{2\pi} + \gamma \to \pi^0\pi^0\gamma$.

The quantum numbers of $A'_{2\pi}$ allow its coupling to the electromagnetic field. Therefore, it can mediate, like the ρ^0 meson, the interaction of neutral hadronic systems with that field or with a $C = -1$ system of charged leptons and photons. However, in contrast to the ρ^0 meson, the coupling to the photon of which is fixed by the hypothesis of vector-meson dominance (VMD) [9], the coupling of $A'_{2\pi}$ to the photon is unknown [10]. In addition, the width of $A'_{2\pi}$ is extremely narrow. It comes out as 1.46×10^{-10} MeV if we take the central value of the measured lifetime (1).

In this paper, we will elaborate on some consequences of the fact that $A'_{2\pi}$ interacts with the electromagnetic field. To this end, we need an estimate of the $A'_{2\pi}$ mass, which is related to the binding energy b by $M = 2m_{\pi^+} - b$.

Assuming pure Coulombic interaction, the binding energy of pionium can be calculated from the hydrogen-atom formula

$$b_n = \frac{m_r \alpha^2}{2n^2}, \tag{2}$$

where m_r is the reduced mass in energy units (used throughout this paper), $\alpha \approx 1/137.036$ is the fine-structure constant, and n is the principal quantum number. Putting $n = 2$ for the first excited state and $m_r = m_{\pi^+}/2$, we get $b = 0.4645$ keV. The strong interactions may shift the energies given by Eq. (2) [11]. As far as we know, there is no experimental or theoretical indication that the binding energies of the ground ($n = 1$) or first excited state ($n = 2$) differ significantly from their Coulombic values (2). Nevertheless, Uretsky and Palfrey considered binding energies even higher than 10 MeV in their analysis [1]. Today we know that pionium decays into two neutral pions, so the binding energy b must be smaller than $2(m_{\pi^+} - m_{\pi^0}) \approx 9.19$ MeV.

In this paper we will consider, besides the Coulombic value $b = 0.4645$ keV, the binding energy of $b = 9$ MeV. We hope that the phenomena we are going to study will be able to decide between these two extreme values.

II. POSSIBLE MANIFESTATION OF $2p$ PIONIUM IN THE $e^+e^- \to \pi^+\pi^-$ PROCESS

Recently, we have succeeded [12] in locating $2p$ kaonium as a bound-state pole in the amplitude of the $e^+e^- \to K^+K^-$ process. The pole corresponding to $2p$ kaonium lies on the real axis in the complex s-plane below the K^+K^- threshold. Our aim here is to find a pole in $e^+e^- \to \pi^+\pi^-$ amplitude that would correspond to $2p$ pionium by fitting the data on the $e^+e^- \to \pi^+\pi^-$ cross section. Our experience with $2p$ kaonium shows that the crucial role in discovering the bound-state pole, which lies below the reaction threshold, is played by the cross section data at low energies, as close to the threshold as possible [12]. Unfortunately, almost all $e^+e^- \to \pi^+\pi^-$ experiments have concentrated on the ρ/ω region or on energies above $\phi(1020)$. The only exception is the *BABAR* experiment [13], which in 2012 covered a wide energy range from 0.3 to 3.0 GeV by exploring the initial-state radiation method [14]. The files containing the cross section data and their covariance matrices are provided in the Supplemental Material repository (Ref. 32 in [13]).

To fit the *BABAR* cross-section data, we use the VMD formula for the cross section of the e^+e^- annihilation into a pseudoscalar meson and its antiparticle with n interfering resonances in the intermediate state

$$\sigma(s) = \frac{\pi\alpha^2}{3s}\left(1 - \frac{4m_P^2}{s}\right)^{\frac{3}{2}} \left| \sum_{i=1}^{n} \frac{R_i e^{\mathrm{i}\delta_i}}{s - M_i^2 - \mathrm{i}M_i\Gamma_i} \right|^2. \tag{3}$$

TABLE I. Parameters of the fits to *BABAR* $\pi^+\pi^-$ data [13] over the full energy range assuming no pole below the threshold (second column) and the $2p$ pionium with the Coulombic binding energy b (third column) or with $b = 9$ MeV (last column).

	No pionium	$b = 0.464$ keV	$b = 9$ MeV
R_1 (GeV^2)	0.7086(31)	0.7114(28)	0.7060(30)
M_1 (GeV)	0.75629(18)	0.75645(21)	0.75646(21)
Γ_1 (GeV)	0.14361(33)	0.14374(36)	0.14377(36)
$R_2 \times 10^3$ (GeV^2)	7.65(28)	7.73(29)	7.74(28)
M_2 (GeV)	0.78203(18)	0.78204(18)	0.78204(18)
Γ_2 (MeV)	8.16(34)	8.23(35)	8.24(34)
δ_2	−2.02(36)	−2.02(37)	−2.02(36)
R_3 (GeV^2)	0.477(17)	0.483(38)	0.476(38)
M_3 (GeV)	1.426(12)	1.414(15)	1.413(15)
Γ_3 (GeV)	0.465(22)	0.456(24)	0.455(23)
δ_3	2.63(13)	2.71(13)	2.74(13)
R_4 (GeV^2)	2.63(13)	0.333(40)	0.328(39)
M_4 (GeV)	1.817(18)	1.810(19)	1.809(18)
Γ_4 (GeV)	0.353(25)	0.333(30)	0.330(29)
δ_4	−1.58(20)	−1.31(25)	−1.26(25)
R_5 (GeV^2)	0.045(24)	0.033(18)	0.032(17)
M_5 (GeV)	2.239(28)	2.239(23)	2.238(22)
Γ_5 (GeV)	0.166(90)	0.126(85)	0.122(78)
δ_5	−0.94(41)	−0.71(48)	−0.66(46)
R_6 (GeV^2)		0.0099(33)	0.0125(43)
M_6 (GeV)		$2m_{\pi^+} - b$	$2m_{\pi^+} - b$
Γ_6 (GeV)		0	0
δ_6		−1.566(64)	1.141(68)
χ^2/NDF	236.7/318	233.5/316	233.4/316
Confidence level	100%	100%	100%

Here, M_i and Γ_i determine the position and width of the ith resonance, respectively. The residuum R_i includes the product of two constants. One characterizes the coupling of the ith resonance to the photon (up to the elementary charge e, which is taken off to form, after squaring, an α in the prefactor) and the other is the coupling of the resonance to the pseudoscalar meson pair. The phases δ_i regulate the interference between the resonances. We put $\delta_1 = 0$.

We first perform our fit over the full *BABAR* energy range assuming five "standard" resonances (ρ, ω, ρ', ρ'', ρ''') [15]. Similarly as it was done in Ref. [13] when fitting the data on the pion form factor, we fit the cross-section data with only diagonal errors. We get a perfect fit in terms of standard χ^2 and the number of free parameters (NDF): $\chi^2/\mathrm{NDF} = 236.7/318$, which implies the confidence level (C.L.) of 100%. This is not good news from the point of searching for pionium, because there is little room for improvement. The parameters of the fit are shown in the second column of Table I.

Then we add two free parameters: the residuum of the assumed $2p$ pionium R_6 and the phase shift δ_6. The width Γ_6 is set to zero because the $A'_{2\pi}$ is a stable entity from the point of view of the $e^+e^- \to \pi^+\pi^-$ reaction.

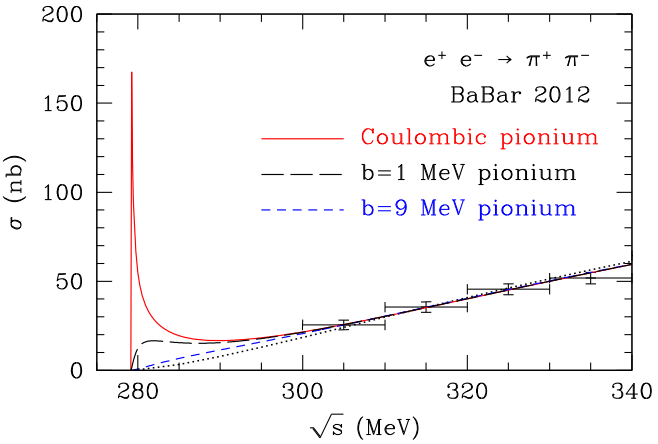

FIG. 1. Low energy parts of the *BABAR* [13] data and of our fit to all (0.3–3.0 GeV) data points. (a) dotted curve: the fit assuming five "standard" resonances; (b) full curve: resonances + Coulombic pionium; (c) long-dash curve: resonances + pionium, $b = 1$ MeV; (d) dashed curve: resonances + pionium, $b = 9$ MeV. Fit parameters are shown (except for the $b = 1$ MeV case) in Table I.

The $2p$ pionium mass is expressed by means of its binding energy b: $M_2 = 2m_{\pi^+} - b$. We consider two cases: (i) $b = 0.464$ keV (Coulombic binding energy), (ii) $b = 9$ MeV. The corresponding fit parameters are shown in the third and fourth column of Table I, respectively. In both cases, the drop of the χ^2 against the case without pionium is more than 3, which with the two more free parameters means that the fitting function has been changed in a sound way. However, it cannot be considered proof of $2p$ pionium existence because a perfect fit also exists without it.

However, even in this situation, something can be learned from the behavior of the calculated cross sections at very low energies depicted in Fig. 1. In the case of $b = 9$ MeV, the excitation curve differs very little from that without pionium and there would be little chance to confirm pionium existence even if the data below 290 MeV were available. A sure sign of the presence of Coulombic (or nearly Coulombic) pionium would be if the lowest 10-MeV-wide bin were taller than the next one. For intermediate binding energies, the sensitivity will depend on the data precision. In Fig. 1, a curve corresponding to $b = 1$ MeV is also depicted.

The origin of the spike in Fig. 1 is obvious. The pole corresponding to Coulombic pionium lies below the threshold, very close (0.464 keV) to it. So the beginning of the slope is already "visible" above the threshold. In the amplitude squared, the rise continues to very high values (to infinity as the Γ_6 is set to zero) at $\sqrt{s} = M_6 < 2m_{\pi^+}$. In the excitation function, the rise is cut off by the p_π^{*3} factor in Eq. (3) and a vanishing cross section is reached at the reaction threshold.

III. POSSIBLE MANIFESTATION OF $2p$ PIONIUM IN THE $V^0 \to \pi^0 \ell^+ \ell^-$ DECAYS

In this section, we will try to spot the traces of $2p$ pionium in the most recent data on the $\omega \to \pi^0 e^+ e^-$ [16], $\omega \to \pi^0 \mu^+ \mu^-$ [17], and $\phi \to \pi^0 e^+ e^-$ [18] decays.

A. Phenomenology

The formula that expresses the differential decay width of a neutral vector meson to a neutral pion and the dilepton with invariant mass M in terms of the decay width of its real photon alternative [19] can be cast in the form

$$\frac{d\Gamma(V^0 \to \pi^0 \ell^+ \ell^-)}{dM^2} = \left(\frac{p_{\gamma_M}}{p_\gamma}\right)^3 \Gamma(V^0 \to \pi^0 \gamma) \times \mathcal{T}(M^2) |F_{V^0\pi^0}(M^2)|^2, \quad (4)$$

where p_{γ_M} (p_γ) is the dilepton (photon) momentum in the V^0 rest frame, $F_{V^0\pi^0}$ is the transition form factor, and

$$\mathcal{T}(M^2) = \frac{\alpha}{3\pi M^2}\left(1 + \frac{2m^2}{M^2}\right)\left(1 - \frac{4m^2}{M^2}\right)^{1/2}. \quad (5)$$

The last function is known [20–22] as providing the connection between the production of the dilepton and a fictitious massive photon γ_M. In our case,

$$\frac{d\Gamma(V^0 \to \pi^0 \ell^+ \ell^-)}{dM^2} = \Gamma(V^0 \to \pi^0 \gamma_M) \times \mathcal{T}(M^2). \quad (6)$$

We can thus write the relation

$$|F_{V^0\pi^0}(M^2)|^2 = \frac{\Gamma(V^0 \to \pi^0 \gamma_M)}{\Gamma(V^0 \to \pi^0 \gamma)} \times \left(\frac{p_\gamma}{p_{\gamma_M}}\right)^3, \quad (7)$$

which will be explored later.

B. The model

There are many interesting theoretical approaches to the $V^0 \to \pi^0 \ell^+ \ell^-$ phenomenon [23]. As we want to concentrate on the role of $2p$ pionium, we will use the simplest possibility—the VMD model, which allows the easy and transparent inclusion of $2p$ pionium into the game. The simplest Lagrangian of the $V^0 \rho^0 \pi^0$ interaction [24]

$$\mathcal{L}(x) = g_{V\rho\pi} \epsilon_{\mu\nu\alpha\beta} \partial^\mu V^\nu(x) \partial^\alpha \rho^\beta(x) \pi(x) \quad (8)$$

and the electromagnetic-current–vector-field identity [9]

$$J_\mu(x) = -\frac{e}{g_\rho} m_\rho^2 \rho_\mu(x)$$

are used to calculate both decay widths on the right-hand side of Eq. (7). In this way we obtain the form factor of the VMD model

$$F_{V^0\pi^0}(s) = \frac{m_\rho^2}{m_\rho^2 - s + \mathrm{i}m_\rho\Gamma_\rho(s)}, \tag{9}$$

where $s = M^2$. The energy-dependent total width of the ρ^0 is given, at energies we will use, by the $\rho^0 \to \pi^+\pi^-$ decay width

$$\Gamma_\rho(s) = \Gamma_\rho \frac{m_\rho^2}{s}\left(\frac{s - 4m_{\pi^+}^2}{m_\rho^2 - 4m_{\pi^+}^2}\right)^{3/2}. \tag{10}$$

The Γ_ρ is the decay width of the ρ^0 at its nominal mass m_ρ.

However, it is known, and recent experiments [16–18] have confirmed, that the VMD model provides a very poor description of the experimental data on the $V^0 \to \pi^0\ell^+\ell^-$ decays. We will therefore modify the VMD model in a way that was suggested in Ref. [25], namely, by taking into account the possible energy dependence of the $V^0 \to \rho^0\pi^0$ vertex by replacing the coupling constant in Eq. (8) by a strong form factor. Inspired by the flux-tube-breaking model of Kokoski and Isgur (KI) [26], we assume that the strong form factor behavior is given by formula

$$G_{V\rho\pi}(p^*) = g_{V\rho\pi} \times \exp\left\{-\frac{p^{*2}}{12\beta^2}\right\}, \tag{11}$$

where p^* is the momentum of either of the particles coming out of the $V^0 \to \rho^0\pi^0$ vertex in the V^0 rest frame. KI estimated the value of parameter β at 0.4 GeV. We will consider it a free parameter.

Applying formula (11) to the decay widths on the right-hand side of Eq. (7), we find that the $|F_{V^0\pi^0}(M^2)|^2$ acquires, in comparison with the standard VMD, an extra factor of

$$K(s) = \exp\left\{\frac{p_\gamma^2 - p_{\gamma_M}^2}{6\beta^2}\right\}.$$

Using $p_{\gamma_M}^2 = \lambda(m_{V^0}^2, m_{\pi^0}^2, s)/(4m_{V^0}^2)$, where the "triangle" function is defined by

$$\lambda(x, y, z) = x^2 + y^2 + z^2 - 2xy - 2xy - 2yz, \tag{12}$$

we end up with

$$K(s) = \exp\left\{\frac{s(2m_{V^0}^2 + 2m_{\pi^0}^2 - s)}{24m_{V^0}^2\beta^2}\right\}.$$

Finally, adding the $2p$ pionium interfering with ρ^0, we arrive at the form factor squared of our model

$$|F_{V^0\pi^0}(s)|^2 = \frac{K(s)}{(1+\epsilon)^2}\left|\frac{m_\rho^2}{m_\rho^2 - s + \mathrm{i}m_\rho\Gamma_\rho(s)} + \epsilon\frac{m_{2\pi}^2}{m_{2\pi}^2 - s + \mathrm{i}m_{2\pi}\Gamma_{2\pi}}\right|^2. \tag{13}$$

The constant ϵ will be treated as a free parameter.

The experimental data are provided as mean values of the form factor squared within bins in M. We therefore produce the model outcome in the same format. It must be said that due to the presence of an extremely narrow resonance in the form factor (13) it would be unthinkable to proceed in a different way, e.g., by calculating the form factor squared in isolated points. Another possible way would be to convolute the model outcome with the M-resolution of a particular experiment.

As the experimental bins are immensely wider than the $2p$ pionium width, the last contributes only to a single bin. For calculating the model outcome in that bin, we use the numerical quadrature method described in the Appendix.

C. Results

1. $\omega \to \pi^0 e^+ e^-$ decay

The A2 Collaboration at Mainz Microtron (MAMI) in 2017 presented the first measurement of the dielectron mass spectrum in the $\omega \to \pi^0 e^+ e^-$ decay. The electron beam from the MAMI-C accelerator produced Bremsstrahlung photons in a radiator. The photons hit a liquid hydrogen target and initiated the $\gamma p \to \omega p$ reaction. The results were presented in the form of the $\omega\pi^0$ transition form factor squared $|F_{\omega\pi^0}|^2$ [16]. Previously, the data on this quantity were only obtained from the dimuon mass spectrum in the $\omega \to \pi^0\mu^+\mu^-$ decay [17,27,28].

Using our model Ansatz (13) without the $\mathrm{A}'_{2\pi}$ contribution ($\epsilon \equiv 0$) we get a very good fit ($\chi^2/\mathrm{NDF} = 0.4/13$) to the A2 data, see Fig. 2. The optimal value of the parameter β is 0.289 ± 0.098 GeV, which is not far from the value of 0.4 GeV suggested by Kokoski and Isgur [26]. When considering our main interest in this paper, the manifestation of $2p$ pionium, the A2 data are not supportive at all. As the mass of $2p$ pionium must lie between $2m_\pi^0$ and $2m_\pi^+$, it would appear in the bin [0.25 GeV, 0.30 GeV]. However, the model value of $|F_{\omega\pi^0}|^2$ in this bin is already higher than the experimental one. Therefore, including $2p$ pionium can only worsen the fit quality.

2. $\phi \to \pi^0 e^+ e^-$

The KLOE experiment at the DAΦNE e^+e^- collider at Frascati, Italy, is the site where historically the first measurement of the dielectron mass distribution in the $\phi \to \pi^0 e^+ e^-$ decay was performed. The results in the form of the $\phi\pi^0$ transition form factor were presented by KLOE-2 Collaboration in Ref. [18].

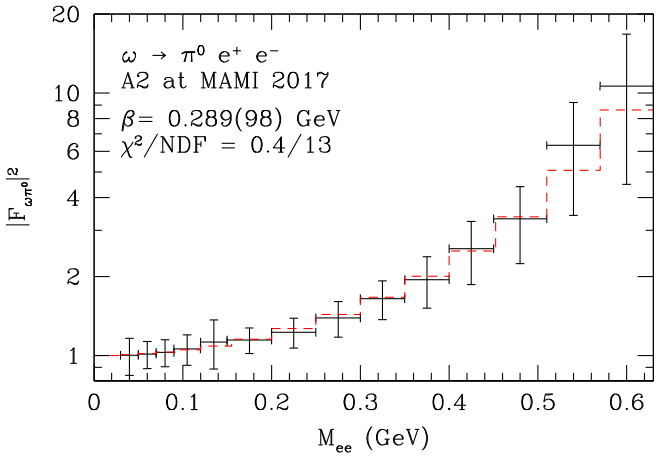

FIG. 2. Fit of our model to the A2 Collaboration at MAMI data [16] on $\omega \to \pi^0 e^+ e^-$ decay. The dashed histogram represents the outcome of the model without the $A'_{2\pi}$ contribution ($\epsilon = 0$). As the model is above the data in the bin [0.25, 0.30] GeV, in which a possible contribution from $A'_{2\pi}$ is expected, a nonvanishing ϵ cannot improve the fit (because of the extreme narrowness and huge peak value of $A'_{2\pi}$, the destructive interference is excluded).

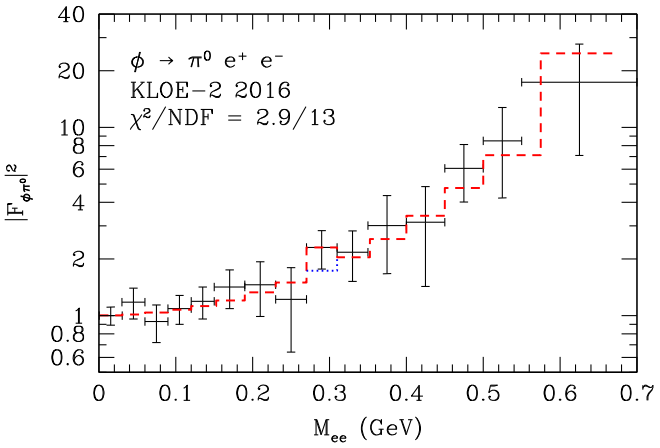

FIG. 3. Comparison of our model with the KLOE-2 data [18]. Model outcome (dashed histogram) is the same for both assumed values of the $2p$ pionium binding energy because both alternative $A'_{2\pi}$ masses fall in the same [0.27, 0.31] GeV bin. In this bin, the model perfectly matches the experimental value thanks to the fitting parameter ϵ, which regulates the contribution of $A'_{2\pi}$ to the form factor squared. The dots in the [0.27, 0.31] GeV bin indicate the form-factor-squared value without the $2p$ pionium contribution.

We fit the KLOE-2 data by our form factor formula (13) using three options: (i) no $2p$ pionium ($\epsilon = 0$), (ii) $2p$ pionium with the Coulombic binding energy of 0.464 keV, and (iii) $2p$ pionium with the binding energy of 9 MeV. The results are listed in Table II and displayed in Fig. 3. The calculated dependence of $|F_{\phi\pi^0}|^2$ on dielectron mass is the same for all three options with one exception: in the bin extending from 0.27 to 0.31 GeV the two options with $2p$ pionium match the experimental value, whereas the option without $A'_{2\pi}$ is somewhat lower. This may be considered an indication of the role of $2p$ pionium in the $\phi \to \pi^0 e^+ e^-$ decay.

However, the enhancement of a single bin in comparison with its neighbors may be a statistical fluctuation. The way to decide whether the enhancement is a real effect or just a fluctuation is to use narrower bins, if the statistics permit. The idea is illustrated in Fig. 4. The imbalance between the two sub-bins is more significant if the original bin contains a $A'_{2\pi}$. In our example, $2p$ pionium falls into the left sub-bin [0.27, 0.29] GeV for both choices of the binding energy. In a high-statistics experiment, it would be possible to get the pionium mass better localized by choosing sufficiently narrow bins.

TABLE II. Parameters of the fits of our model to the KLOE-2 Collaboration data [18] on $\phi \to \pi^0 e^+ e^-$ decay.

	No pionium	$b = 0.464$ keV	$b = 9$ MeV
$\epsilon \times 10^7$	0 (fixed)	1.49(72)	1.55(74)
β (GeV)	0.168(21)	0.174(25)	0.174(25)
χ^2/NDF	4.0/14	2.9/13	2.9/13
Confidence level	99.5%	99.8%	99.8%

3. $\omega \to \pi^0 \mu^+ \mu^-$

The NA60 Collaboration studied the $\omega \to \pi^0 \mu^+ \mu^-$ decays in two experiments performed at the CERN SPS. In the first experiment [28], the ω mesons were produced in 158A GeV In-In collisions. In the second one [17], a system of nine subtargets of different nuclear species

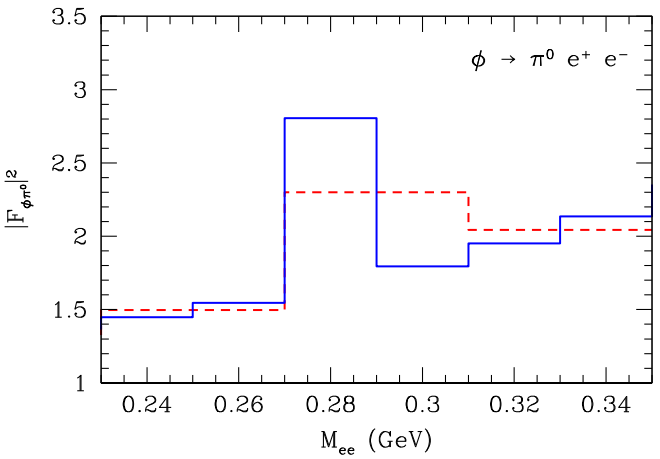

FIG. 4. The original histogram (a part of that shown in Fig. 3) (dashed) and a histogram with narrower bins (full). Illustrating the idea that by dividing a bin into two sub-bins one can decide whether it contains the contribution from a narrow resonance or not. Of the three displayed bins, splitting the middle one provides two sub-bins with very different contents because the resonance position falls into the left sub-bin. In two side bins, the difference between sub-bins is not so pronounced, they do not contain a resonance.

TABLE III. Parameters of the fits of our model to the NA60 Collaboration data [17] on $\omega \to \pi^0\mu^+\mu^-$ decay for $M_{\mu\mu} < 0.48$ GeV.

	No pionium	$b = 0.464$ keV	$b = 9$ MeV
$\epsilon \times 10^7$	0 (fixed)	0.63(52)	0.65(54)
β (GeV)	0.227(24)	0.228(25)	0.228(25)
χ^2/NDF	7.5/13	7.1/12	7.1/12
Confidence level	87.5%	85.1%	85.1%

was exposed to an incident 400 GeV proton beam. The results of the two experiments are compatible [17]. We will only use the results of the latter experiment, presented as the mean values of the $\omega\pi^0$ transition form factor squared in 20 MeV-wide dimuon mass bins.

Unfortunately, our model is not able to fit the data over the whole range of dimuon masses from 0.20 to 0.64 GeV. Not only our model, but also all the models investigated in Ref. [17] are unable to follow a steep rise of the form factor above 0.5 GeV found in both NA60 experiments. A similar rise was reported by the Lepton G experiment [27] performed at the Institute for High Energy Physics, Serpukhov, Russia, in 1981.

To have a good fit in the region around the possible occurrence of the $A'_{2\pi}$, we do not include the dimuon masses greater than 0.48 GeV in our fits. The parameters of our three fits (no pionium, Coulombic binding, binding energy of 9 MeV) are shown in Table III.

When producing a graphical output (Fig. 5) our task has again been facilitated by the fact that outside the [0.26, 0.28] GeV bin all three fits give the same histogram. In that bin, the two $2p$ pionium options give identical results, the option without pionium gives a somewhat lower value.

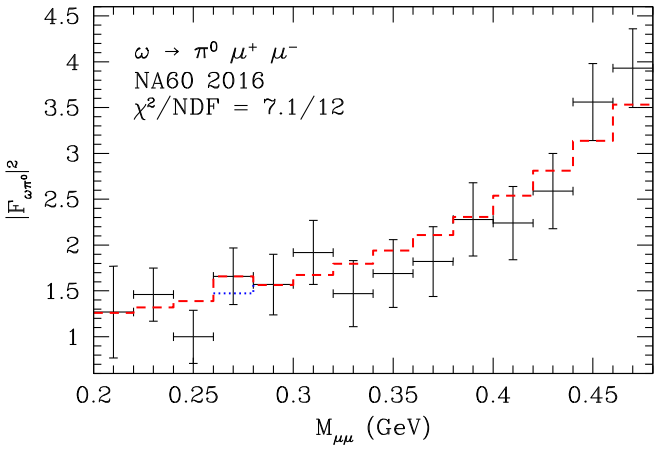

FIG. 5. Comparison of our model with the NA60 [17] data. The model outcome (dashed histogram) is the same for both assumed values of the $2p$ pionium binding energy because both alternative $A'_{2\pi}$ masses fall in the same [0.26, 0.28] GeV bin. In this bin, the model perfectly matches the experimental value thanks to the fitting parameter ϵ, which regulates the contribution of $A'_{2\pi}$ to the form factor squared. The dots in the [0.26, 0.28] GeV bin indicate the form factor squared value without the $2p$ pionium contribution.

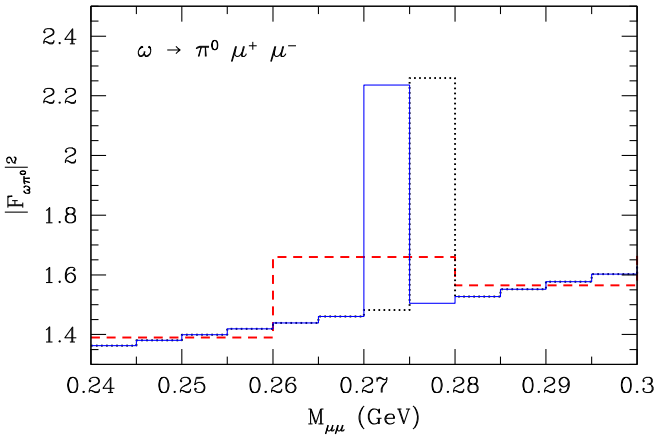

FIG. 6. Dashed line: a part of the original histogram shown in Fig. 5); Solid line: the calculation assuming a 9 MeV binding energy of $2p$ pionium; Dotted line: $2p$ pionium with Coulombic binding energy. Parameters β and ϵ are kept at values shown in Table III.

The bin width in the NA60 data is 20 MeV. To model what would happen if a narrower bin width were chosen, we first set it to 10 MeV and got a similar picture as in the KLOE-2 case (Fig. 4), just the role of sub-bins was exchanged (in the NA60 case the right sub-bin is taller than the left one). More interesting is the case with the bin width of 5 MeV, see Fig. 6. Now, two binding energy options produce two different histograms. The mass of the Coulomb-bound $A'_{2\pi}$ is in the [0.275, 0.280] GeV bin, whereas the mass of that with $b = 9$ MeV lies in the [0.270, 0.275] GeV bin.

IV. POSSIBLE MANIFESTATION OF $2p$ PIONIUM IN THE $K^\pm \to \pi^\pm\ell^+\ell^-$ DECAYS

The decays $K^\pm \to \pi^\pm\ell^+\ell^-$ have been examined in several experiments [29]. We will use the e^+e^- and $\mu^+\mu^-$ data from the NA48/2 experiment [30,31], which are available in tabular form.

Below, we will show that the NA48/2 experiment does not provide any indication about the existence of the $A'_{2\pi}$ with Coulombic binding. The evidence of the existence of $A'_{2\pi}$ with a higher binding energy (we consider 9 MeV, but somewhat smaller values are also possible) is stronger.

A. Phenomenology

The experimental data on the differential decay rate are most often presented in terms of the dimensionless variable $z = M^2/m_K^2$, where M is the invariant dilepton mass, $M^2 = (p_{\ell^+} + p_{\ell^-})^2$, and m_K is the charged kaon mass [32]. To get the model yield in a particular z-bin, one needs to calculate the integral of $d\Gamma/dz$. In the presence of a

narrow resonance, it is more convenient to calculate the integral of $d\Gamma/dM$ (see Appendix) and use

$$\int_{z_1}^{z_2} \frac{d\Gamma}{dz} dz = \int_{M(z_1)}^{M(z_2)} \frac{d\Gamma}{dM} dM$$

Using the model-independent formula for $d\Gamma/dz$ valid in the one-photon approximation [33,34] and the relation $dz/dM = 2M/m_K^2$, we arrive at the formula

$$\frac{d\Gamma}{dM} = \frac{G_F^2 \alpha^2 m_K^3}{6\pi(4\pi)^4} M \lambda^{\frac{3}{2}}(1, M^2/m_K^2, m_\pi^2/m_K^2) \times \sqrt{1-4\frac{m_\ell^2}{M^2}}\left(1+2\frac{m_\ell^2}{M^2}\right)|f(M^2)|^2, \quad (14)$$

where function λ is defined in Eq. (12). A particular model is defined by specifying the (unnormalized) form factor $f(M^2)$.

The prefactor on the right-hand side of Eq. (14) is chosen in such a way that $f(0) = f_0$, where f_0 is the parameter used by the NA48/2 Collaboration in their papers [30,31].

B. Model

We will use a model based on meson dominance (MD) hypothesis [35] depicted in Fig. 7, supplemented with $2p$ pionium interfering with the ρ^0 in the intermediate state. It was shown that the MD model can provide a reasonable estimate of the $K^+ \to \pi^+ e^+ e^-$ decay rate using the information about the $\tau^+ \to \bar{\nu}_\tau \pi^+ \pi^+ \pi^-$ and $K^+ \to \mu^+ \nu_\mu$ decay rates [25,35]. But it failed in explaining the $K^+ \to \pi^+ \mu^+ \mu^-$ to $K^+ \to \pi^+ e^+ e^-$ branching ratio and the dilepton mass distribution shape, even when the KI strong form factor [26] was taken into account [25]. Also here, we will replace the $a_1 \rho \pi$ coupling constant by an energy-dependent form factor

$$G_{a_1\rho\pi}(p^*) = g_{a_1\rho\pi} \times \exp\left\{-\frac{p^{*2}}{12\beta^2}\right\}, \quad (15)$$

where p^* is the 3-momentum of either of the particles coming out of the $a_1 \to \rho\pi$ vertex in the a_1 rest frame. However, there is a catch. The relation (15) from the flux-tube breaking model [26] is valid when the parent meson is on the mass shell $p_{a_1}^2 = m_{a_1}^2$. In the MD model of the $K^\pm \to \pi^\pm \ell^+ \ell^-$ decay, visualized in Fig. 7, the a_1 meson is off the mass shell, $p_{a_1}^2 = m_K^2$. We will make an additional assumption that the relation (15) holds also in this case. It results in diminishing the form factor in (14) by ($s = M^2$)

$$L(s) = \exp\left\{\frac{s(2m_K^2 + 2m_\pi^2 - s)}{48 m_K^2 \beta^2}\right\}. \quad (16)$$

Contrary to Ref. [25], we will not use the KI value of $\beta = 0.4$ GeV (valid for the on-mass-shell parent mesons) but will consider β a free parameter. Adding the $A'_{2\pi}$ interfering with the ρ^0 in the intermediate state and putting all pieces together we get

$$f(s) = f_0 F(s), \quad (17)$$

with the normalized form factor equal to

$$F(s) = \frac{L(s)}{(1+\epsilon)}\left[\frac{m_\rho^2}{m_\rho^2 - s + i m_\rho \Gamma_\rho(s)} + \epsilon \frac{m_{2\pi}^2}{m_{2\pi}^2 - s + i m_{2\pi}\Gamma_{2\pi}}\right]. \quad (18)$$

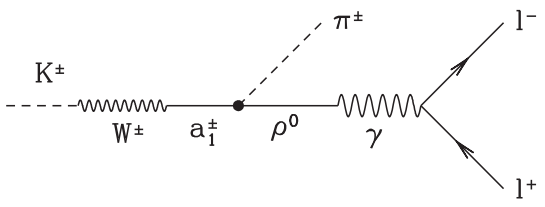

FIG. 7. Meson dominance model [35] of the $K^\pm \to \pi^\pm \ell^+ \ell^-$ decay.

C. Results

1. $K^\pm \to \pi^\pm e^+ e^-$

The NA48/2 experiment at the CERN SPS used simultaneous K^+ and K^- beams produced by 400 GeV/c proton impinging on a beryllium target. After momentum selection and focusing, the beams entered the fiducial decay volume with a length of 114 m. The decay products were registered and measured by the very complex NA48 detector. The results based on the data set collected in 2003-2004 included the rates, spectra, and charge asymmetry. They were presented in 2009 [30]. We will use the dielectron z-spectrum in tabular form, which can be found in [36].

We first fit the full z-spectrum (21 points) with the MD model without $2p$ pionium ($\epsilon \equiv 0$). See the leftmost data column in Table IV and Fig. 8. After including any of the two $2p$ pioniums, the histogram remains the same as in Fig. 8 except the bin where a particular pionium sits. In that bin, a perfect match with data is reached by varying parameter ϵ. As the confidence levels in Table IV show,

TABLE IV. Results of the fits of the MD model to the NA48/2 data [30] on $K^\pm \to \pi^\pm e^+ e^-$ decay.

	No pionium	$b = 0.464$ keV	$b = 9$ MeV
$\epsilon \times 10^7$	0 (fixed)	0.30(14)	0.512(91)
β (GeV)	0.0909(28)	0.0916(30)	0.0924(30)
f_0	0.5622(96)	0.5635(97)	0.5646(98)
χ^2/NDF	23.9/19	22.7/18	15.8/18
Confidence level	20.0%	20.2%	60.6%

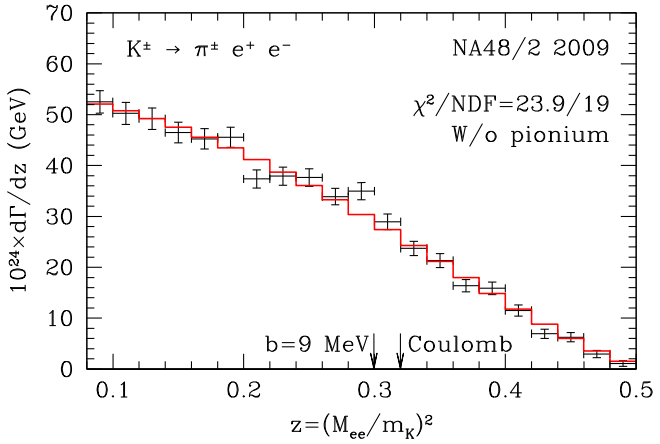

FIG. 8. Fit of the modified MD model to the NA48/2 data. No pionium is included. The arrows show the assumed z-positions of the $2p$ pionium with binding energy of 9 MeV and of that with Coulombic binding energy.

the NA48/2 data prefer the $2p$ pionium with higher binding energy. This is also visible in Fig. 8, where the data point is well above the model in bin $z \in [0.28, 0.30]$. In Fig. 9 we show the detailed histogram stemming from the model with the $b = 9$ MeV $2p$ pionium added. The histogram with the same bin width as in experimental data is shown by a dashed line (now, the experimental value is exactly matched). The dotted line shows the calculated half-width histogram. It suggests the way experimentalists may decide whether an excess over the model without pioniums (or in comparison with neighboring bins) is a statistical fluctuation or a sign of $2p$ pionium presence.

The contribution of a narrow resonance does not depend much on its exact z position within a bin. Inspecting Fig. 9 we can say that any $2p$ pionium with a z position less than 0.3 would have the same effect as that with $b = 9$ MeV. In terms of binding energy it means that any $A'_{2\pi}$ with

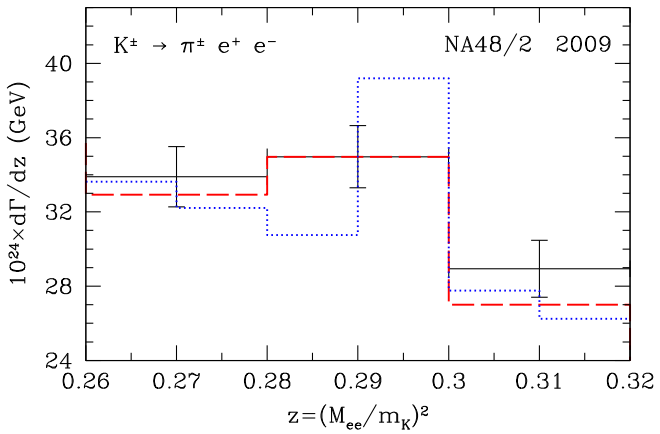

FIG. 9. Detail of the fit to the NA48/2 data after the $2p$ pionium with binding energy of 9 MeV has been included (dashed histogram). The model expectation with narrower bins is also shown (dotted histogram).

TABLE V. Results of the fits of the modified MD model to the NA48/2 data [31] on $K^{\pm} \to \pi^{\pm}\mu^{+}\mu^{-}$ decay.

	No pionium	$b = 0.464$ keV	$b = 9$ MeV
$\epsilon \times 10^7$	0 (fixed)	0.14(36)	0.33(16)
β (GeV)	0.0857(61)	0.0859(63)	0.0863(63)
f_0	0.544(28)	0.544(29)	0.545(29)
χ^2/NDF	13.4/15	13.4/14	12.3/14
Confidence level	57.1%	49.5%	58.2%

$b > 8.78$ MeV are acceptable. When taking into account the higher bound given by the $m_{\pi^+} - m_{\pi^0}$ difference, we can say that the e^+e^- data of the NA48/2 Collaboration confine the $2p$ pionium binding energy to a narrow interval $b \in (8.78, 9.19)$ MeV.

2. $K^{\pm} \to \pi^{\pm}\mu^{+}\mu^{-}$

The measurement of the $K^{\pm} \to \pi^{\pm}\mu^{+}\mu^{-}$ decay based on the data collected by the NA48/2 experiment at the CERN SPS was reported in Ref. [31]. The numerical values of the presented z-distribution are available at [37].

The results of our fits are shown in Table V. The model without any pionium ($\epsilon = 0$) exhibits a very good fit (C.L. of 62.5%). The histogram showing the corresponding z-distribution is depicted in Fig. 10.

In the bin $z \in [0.30, 0.32]$, where the Coulombic $A'_{2\pi}$ resides, the model and experimental values almost coincide. There is no room for the improvement of χ^2 by allowing nonvanishing ϵ. Thus, the $\mu^+\mu^-$ mode does not allow the presence of the $2p$ pionium with Coulombic binding energy.

The $A'_{2\pi}$ with $b = 9$ MeV is less salient than in the e^+e^- mode. Its inclusion improves the confidence level only marginally. Additionally, the value of the parameter that

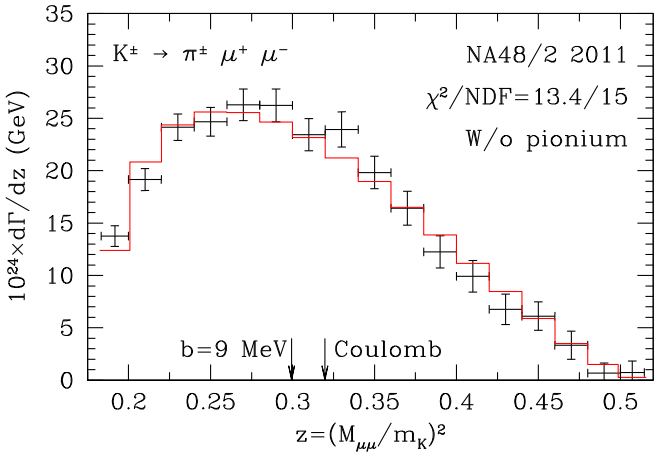

FIG. 10. Fit of the modified MD model to the NA48/2 data. No pionium is included. The arrows show the assumed z-positions of the $2p$ pionium with binding energy of 9 MeV and that with Coulombic binding energy.

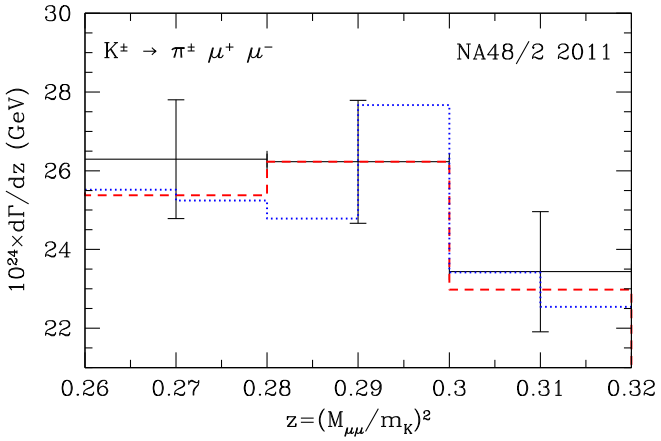

FIG. 11. Detail of the fit to the NA48/2 data after the $2p$ pionium with binding energy of 9 MeV has been included (dashed histogram). The model expectation with narrower bins is also shown (dotted histogram).

characterizes the admixture of $A'_{2\pi}$ in the form factor (18) ($\epsilon = 0.33 \pm 0.16$) is smaller than that in Table IV (0.512 ± 0.091). Nevertheless, Fig. 11 again illustrates that narrower bins may help to identify the z-position of the resonance.

V. PHOTOPRODUCTION OF $A'_{2\pi}$ FROM NUCLEONS

A long time ago [1], the photoproduction reaction

$$\gamma + p \to b^0 + p$$

was considered a convenient means of detecting the scalar $\pi^+\pi^-$ atom b^0 ($A_{2\pi}$, in today's notation). None of the numerous experiments, starting with the bubble chamber experiments at Cambridge, DESY, and at SLAC in the 1960s, and continuing with many electronic experiments to the present day (see [38] for a list of the most recent ones), has had a glimpse of pionium. Most probably this is because ground-state pionium does not couple to an electromagnetic field. On the other hand, $2p$ pionium can be produced in inelastic Compton scattering, where it directly couples to the outgoing virtual photon. However, $2p$ pionium exhibits special properties, which should be taken into account. Its most salient feature is the long lifetime (1), which means a long decay length. For example, if an event is initiated by a photon with energy $E_\gamma = 1$ GeV, the maximum $A'_{2\pi}$ momentum is 0.959 GeV/c and the corresponding decay length is 4.6 mm. So, the $A'_{2\pi}$ events will have a two-vertex structure, with separation between vertices of a few millimeters. In the first vertex, the target proton gets a kick against the emitted $2p$ pionium, while two π^0s and a very soft photon appear from the decay chain $A'_{2\pi} \to A_{2\pi} + \gamma \to \pi^0\pi^0\gamma$ in the second vertex. The four-momenta of the four energetic γ quanta (coming from two π^0's) should combine to the invariant mass of $A_{2\pi}$, which is a little below $2m_{\pi^+}$.

Even if the current photoproduction experiments are devoted to the study of nucleon resonances, the by-product of an independent confirmation of the existence of long-lived pionium, discovered in [8], and getting its lifetime would be very valuable.

VI. CONCLUSIONS

The message from available experimental data about the appearance of $2p$ pionium is mixed:

The $e^+e^- \to \pi^+\pi^-$ process, even if supplemented with the cross section data closer to the threshold, would only be able to reject or confirm a low-binding-energy ($\lesssim$1 MeV) $A'_{2\pi}$, but would not be able to say anything about those with higher binding energy.

As of $V^0 \to \pi^0\ell^+\ell^-$ decays, the A2 Collaboration data [16] on $\omega \to \pi^0 e^+e^-$ decay provide no room for $A'_{2\pi}$. The experimental value of the form factor squared in the bin where $2p$ pionium is expected is higher than the model result without pionium. What concerns the decays $\omega \to \pi^0\mu^+\mu^-$ (NA60 [17] and $\phi \to \pi^0 e^+e^-$ (KLOE-2 [18]) they exhibit very similar behavior. For each of them, the confidence levels of the three fit options (no pionium, Coulombic pionium, pionium with $b = 9$ MeV) are the same. There is some room for pionium with any binding energy, the parameter ϵ, which measures the $A'_{2\pi}$ contribution to the form factor is not vanishing, but with low statistical significance.

The strongest indication of the $A'_{2\pi}$ presence is provided by the $K^\pm \to \pi^\pm e^+e^-$ data [30] of NA48/2 Collaboration. While the fit with no pionium gives C.L. of 20.2%, the inclusion of $2p$ pionium with $b = 9$ MeV increases C.L. to 60.6% and leads to $\epsilon = (0.512 \pm 0.091) \times 10^{-7}$. Evidence for the Coulombic bound $A'_{2\pi}$ is very weak. Similar, but not so impressive, results are obtained by analyzing the NA48/2 data on the $K^\pm \to \pi^\pm\mu^+\mu^-$ process [31].

The photoproduction data [38] exhibit a steep rise of the $\pi^0\pi^0$ mass spectrum above the threshold, but it is unclear to which extent it signals the presence of $A'_{2\pi}$. A dedicated analysis of the measured data would be useful, taking into account the specific features of possible $A'_{2\pi}$ production events.

A final remark concerns two rare kaon decay experiments KOTO [39] and NA62 [40]. Decays $K \to \pi A_{2\pi}$ and $K \to \pi A'_{2\pi}$ may constitute a part of the background to the main investigated decay $K \to \pi\nu\bar{\nu}$ [41]. While the decay $K^\pm \to \pi^\pm A_{2\pi}$ has already been discovered [6], the decays $K^\pm \to \pi^\pm A'_{2\pi}$, $K_L \to \pi^0 A_{2\pi}$, and $K_L \to \pi^0 A'_{2\pi}$ are still awaiting observation.

ACKNOWLEDGMENTS

I am indebted to Evelina Mihova Gersabeck and Michal Koval for useful correspondence. This work was partly supported by the Ministry of Education, Youth and Sports

of the Czech Republic Inter-Excellence Projects No. LTI17018 and No. LTT17018.

APPENDIX: INTEGRATING OVER THE INTERVAL CONTAINING A NARROW RESONANCE

When comparing the model results with the experimental data presented as mean values over the finite bins we need to calculate the expressions of the type

$$I = \int_{W_1}^{W_2} g(W)\mathrm{d}W. \tag{A1}$$

If the function $g(W)$ contains a narrow-resonance term

$$\frac{1}{(W^2 - M^2)^2 + (M\Gamma)^2}$$

$(W_1 < M < W_2)$, the numerical quadrature may be rather erratic. Using the substitution

$$W(\xi) = M + \frac{\Gamma}{2}\tan\left[\frac{a_2 - a_1}{2}\xi + \frac{a_2 + a_1}{2}\right],$$

where

$$a_i = \arctan\frac{2(W_i - M)}{\Gamma}$$

$(i = 1, 2)$ we arrive at the expression

$$I = \frac{a_2 - a_1}{\Gamma}\int_{-1}^{1} g[W(\xi)]\left[(W(\xi) - M)^2 + \frac{\Gamma^2}{4}\right]\mathrm{d}\xi, \tag{A2}$$

which can be conveniently evaluated by the Gauss-Legendre method. It is also convenient to split a wider bin to a part (preferably symmetric around M) that contains the resonance and to the rest, which can be handled by standard quadrature methods.

[1] J. Uretsky and J. Palfrey, Phys. Rev. **121**, 1798 (1961).
[2] L. G. Afanasyev *et al.*, Phys. Lett. B **308**, 200 (1993); **338**, 478 (1994).
[3] B. Adeva *et al.*, Phys. Lett. B **619**, 50 (2005); Nucl. Instrum. Methods Phys. Res., Sect. A **515**, 467 (2003); Phys. Lett. B **704**, 24 (2011).
[4] H. Jallouli and H. Sazdjian, Phys. Rev. D **58**, 014011 (1998); **58**, 099901(E) (1998); M. A. Ivanov, V. E. Lyubovitskij, E. Z. Lipartia, and A. G. Rusetsky, ibid. **58**, 094024 (1998); J. Gasser, V. E. Lyubovitskij, A. Rusetsky, and A. Gall, ibid. **64**, 016008 (2001).
[5] J. Gasser, V. E. Lyubovitskij, and A. Rusetsky, Phys. Rep. **456**, 167 (2008).
[6] J. R. Batley *et al.* (NA48/2 Collaboration), Phys. Lett. B **633**, 173 (2006).
[7] An alternative formulation in terms of $\pi^+\pi^- \to \pi^0\pi^0$ rescattering was suggested by N. Cabibbo Phys. Rev. Lett. **93**, 121801 (2004).
[8] B. Adeva *et al.*, Phys. Lett. B **751**, 12 (2015); Phys. Rev. Lett. **122**, 082003 (2019).
[9] Y. Nambu and J. J. Sakurai, Phys. Rev. Lett. **8**, 79 (1962); **8**, 191(E) (1962); M. Gell-Mann, D. Sharp, and W. Wagner, ibid. **8**, 261 (1962).
[10] In principle, the $\gamma - 2p$ pionium coupling constant may be measured in the Bhabha ($e^+e^- \to e^+e^-$) scattering or in the $e^+e^- \to \mu^+\mu^-$ annihilation at energies below the $\pi^+\pi^-$ threshold.
[11] J. Gasser, V. E. Lyubovitskij, and A. Rusetsky, Annu. Rev. Nucl. Part. Sci. **59**, 169 (2009).
[12] P. Lichard, Phys. Rev. D **101**, 111501(R) (2020).
[13] J. P. Lees *et al.* (*BABAR* Collaboration), Phys. Rev. D **86**, 032013 (2012).
[14] A. B. Arbuzov, E. A. Kuraev, N. P. Merenkov, and L. Trentadue, J. High Energy Phys. 12 (1998) 009; S. Binner, J. H. Kühn, and K. Melnikov, Phys. Lett. B **459**, 279 (1999); M. Benayoun, S. I. Eidelman, V. N. Ivanchenko, and Z. K. Silagadze, Mod. Phys. Lett. A **14**, 2605 (1999).
[15] As always, we find the program MINUIT by F. James and M. Roos, Comput. Phys. Commun. **10**, 343 (1975) to be extremely useful.
[16] P. Adlarson *et al.* (A2 Collaboration at MAMI), Phys. Rev. C **95**, 035208 (2017).
[17] R. Arnaldi *et al.* (NA60 Collaboration), Phys. Lett. B **757**, 437 (2016).
[18] A. Anastasi *et al.* (KLOE-2 Collaboration), Phys. Lett. B **757**, 362 (2016).
[19] C.-H. Lai and C. Quigg, Fermi National Accelerator Report No. FN-296, 1976 (unpublished); L. G. Landsberg, Phys. Rep. **128**, 301 (1985); A. Faessler, C. Fuchs, and M. I. Krivoruchenko, Phys. Rev. C **61**, 035206 (2000).
[20] N. M. Kroll and W. Wada, Phys. Rev. **98**, 1355 (1955).
[21] V. N. Baier and V. A. Khoze, Zh. Eksp. Teor. Fiz. **48**, 946 (1965) [Sov. Phys. JETP **21**, 629 (1965)].
[22] An alternative derivation can be found in P. Lichard, Acta Phys. Slovaca **49**, 215 (1999).
[23] W. Qian and B.-Q. Ma, Eur. Phys. J. C **65**, 457 (2010); C. Terschlüsen and S. Leupold, Phys. Lett. B **691**, 191 (2010); C. Terschlüsen, S. Leupold, and M. F. M. Lutz, Eur. Phys. J. A **48**, 190 (2012); S. Ivashyn, Probl. At. Sci. Technol. **2012N1**, 179 (2012); S. P. Schneider, B. Kubis, and F. Niecknig, Phys. Rev. D **86**, 054013 (2012); F. Niecknig, B. Kubis, and S. P. Schneider, Eur. Phys. J. C **72**, 2014 (2012); B. Ananthanarayan, I. Caprini, and B.

Kubis, ibid. **74**, 3209 (2014); I. Caprini, Phys. Rev. D **92**, 014014 (2015); T. Husek and S. Leupold, Eur. Phys. J. C **75**, 586 (2015); I. V. Danilkin, C. Fernández-Ramírez, P. Guo, V. Mathieu, D. Schott, M. Shi, and A. P. Szczepaniak, Phys. Rev. D **91**, 094029 (2015); B. Ananthanarayan, I. Caprini, and B. Kubis, Int. J. Mod. Phys. A **31**, 1630020 (2016).

[24] U.-G. Meissner, Phys. Rep. **161**, 213 (1988).

[25] P. Lichard, Phys. Rev. D **60**, 053007 (1999).

[26] R. Kokoski and N. Isgur, Phys. Rev. D **35**, 907 (1987).

[27] R. I. Dzhelyadin *et al.*, Phys. Lett. **102B**, 296 (1981).

[28] R. Arnaldi *et al.* (NA60 Collaboration), Phys. Lett. B **677**, 260 (2009).

[29] P. Bloch *et al.*, Phys. Lett. **56B**, 201 (1975); C. Alliegro *et al.*, Phys. Rev. Lett. **68**, 278 (1992); S. Adler *et al.*, ibid. **79**, 4756 (1997); R. Appel *et al.*, ibid. **83**, 4482 (1999); H. Ma *et al.*, ibid. **84**, 2580 (2000); H. K. Park *et al.* (HyperCP Collaboration), ibid. **88**, 111801 (2002).

[30] J. R. Batley *et al.* (NA48/2 Collaboration), Phys. Lett. B **677**, 246 (2009).

[31] J. R. Batley *et al.* (NA48/2 Collaboration), Phys. Lett. B **697**, 107 (2011).

[32] NA48/2 Collaboration used notation M_K, which often means the mean mass of the kaon doublet. The charged kaon mass assignment was confirmed [E. Mihova Gersabeck (private communication)].

[33] G. Ecker, A. Pich, and E. de Rafael, Nucl. Phys. **B291**, 692 (1987).

[34] G. D'Ambrosio, G. Ecker, G. Isidori, and J. Portelés, J. High Energy Phys. 08 (1998) 004.

[35] P. Lichard, Phys. Rev. D **55**, 5385 (1997).

[36] https://www.hepdata.net/record/ins815724.

[37] https://www.hepdata.net/record/ins878312.

[38] M. Dieterle *et al.* (A2 Collaboration), Phys. Rev. Lett. **125**, 062001 (2020).

[39] J. K. Ahn *et al.* (KOTO Collaboration), Phys. Rev. Lett. **122**, 021802 (2019).

[40] E. Cortina Gil *et al.* (NA62 Collaboration), Phys. Lett. B **791**, 156 (2019).

[41] P. Lichard, arXiv:2006.02969.